# Potential of low carbon materials facing biodeterioration in concrete biogas structures

Marie Giroudon, Cédric Patapy, Matthieu Peyre Lavigne, Mialitiana Andriamiandroso, Robin Cartier, Céline Bacquié, Simon Dubos, Ludovic André, Sébastien Pommier, Xavier Lefevbre, et al.

# Potential of low carbon materials facing biodeterioration in concrete biogas structures

Marie Giroudon[1,2], Cédric Patapy[1], Matthieu Peyre Lavigne[2], Mialitiana Andriamiandroso[1], Robin Cartier[1], Simon Dubos[2], Céline Bacquié[1,3], Ludovic André[1,3], Sébastien Pommier[2], Xavier Lefevbre[2], Martin Cyr[1], Alexandra Bertron[1]

[1] LMDC, Université de Toulouse, UPS, INSA, Toulouse, France

[2] TBI, Université de Toulouse, CNRS, INRA, INSA, Toulouse, France

[3] ECOCEM Materials, Paris, France

## Keywords:

Anaerobic digestion

Biodeterioration

Cementitious binders

Low carbon binders

Durability

Biogas production

## Graphical abstract

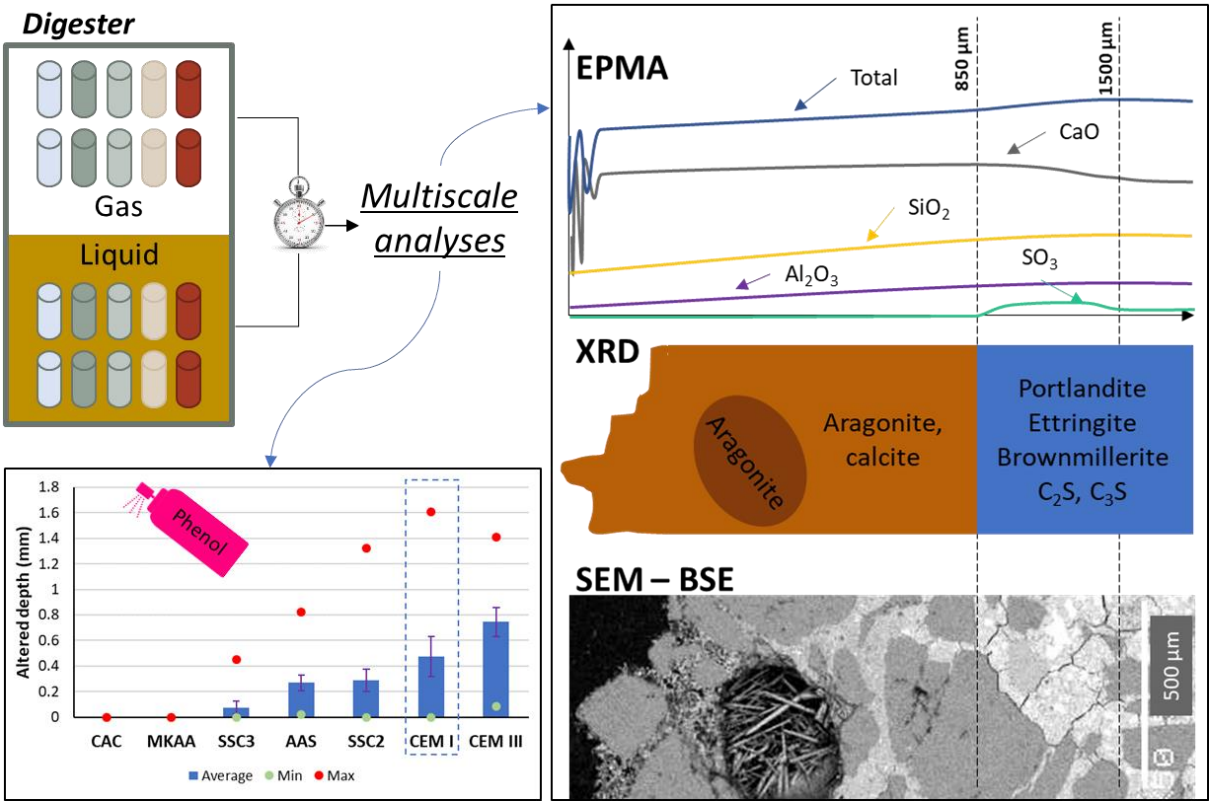

## Abstract

Anaerobic digestion, a renewable energy source, is the degradation of organic waste into biogas, mainly composed of $CH_4$ and $CO_2$. The sector is expanding rapidly due to its multiple environmental and economic benefits. This process is implemented industrially in concrete structures that are in direct contact with the biowaste being digested and the gas produced. Both phases can damage concrete through (i) the presence of volatile fatty acids, dissolved $CO_2$, ammonium, and microbial biofilm in the liquid phase, and (ii) high concentrations of $CO_2$ and various concentrations of $H_2S$ in the gas phase. In order to develop more sustainable concrete biogas units, long-term, in-situ experiments were carried out in a semi-industrial scale digester to provide new insights into the performance levels and deterioration mechanisms of various low-$CO_2$ binders, including alkali-activated metakaolin (geopolymer), alkali-activated slag (AAS), and supersulfated cements (SSC), in comparison to calcium aluminate cement (CAC) and Portland cement based matrices. In the running conditions explored, carbonation of the cementitious matrices was predominant over other deterioration phenomena in both the digester liquid and the gas phases. Alkali-activated metakaolin and calcium aluminate cement performed better with few degradations observed. Supersulfated cements and alkali-activated slag showed an intermediate behaviour with good performance in the acidic liquid phase but low performance in the $CO_2$-rich gas phase.


## Introduction

Anaerobic digestion is a bioprocess transforming organic matter, such as food or agricultural waste, into a renewable energy through the action of microorganisms, in anaerobic conditions. This bioprocess produces biogas mainly composed of $CO_2$ (20% to 50%) and $CH_4$ (50% to 70%), and digestate, generally used as an agricultural amendment [1].

Anaerobic digestion treatment units are mainly made of concrete because this material is not only easy to implement and economical but is also waterproof and airtight, and has good thermal inertia. In digesters, concrete is in contact with the fermenting biowaste and also possibly with the gas produced by the bioprocess, since the liners covering the upper walls [2] may possibly peel off or be punctured. In the liquid phase, microorganisms produce intermediate metabolites such as volatile fatty acids (VFA), dissolved $CO_2$ and $NH_4^+$ ions (produced during acidogenesis and/or contained in some waste [3]), which are aggressive to concrete. The reaction of these metabolites with the hydrated binders leads to the dissolution of its initial phases, a partial decalcification, a loss of density, and secondary precipitation of calcium carbonates [4–9]. Moreover, the presence of microbial biofilm on the concrete surface can locally accentuate the intensity of damage and the kinetics of degradation [5,10,11] through the generation of locally high concentrations of aggressive metabolites. In the gas phase, the very high proportion of carbon dioxide ($CO_2$) associated with the high relative humidity (RH) inside the digester, between 53% and 90% according to Obileke et al. [12], is favourable to the carbonation of the cement phases (carbonation kinetics is maximum for RH between 40% and 80% [13]). Moreover, biogas also contains hydrogen sulphide ($H_2S$), which is known to cause biogenic acid attack of concrete in sewer networks due to the formation of sulfuric acid biologically produced in the presence of oxygen [14–19]. During anaerobic digestion, the gas phase does not normally contain oxygen. However, the digesters

can be opened during the emptying of liquid-state digesters or for the reloading of solid-state digesters. Thus, the structures are actually subjected to alternate anaerobic/aerobic conditions. Also, Koenig and Dehn [6] identified concrete damage caused by sulfuric acid in a digester where desulfurization was carried out using atmospheric oxygen.

If the sustainable development of the rapidly expanding biogas sector is to be ensured, there is a need to develop durable, environmentally friendly concrete structures for biogas production units. To date, very little information is available in the literature on the performance of traditional and low-carbon binders in these environments under real-life conditions. Ordinary Portland cement (OPC), blast furnace slag cement, calcium aluminate cement and metakaolin-based geopolymer have already been tested in laboratory conditions [4,5,8,9,20], while Portland-based cements (OPC, OPC with additions, slag cement) have been exposed in situ [6]. In this context, the present work aims to evaluate the durability of several binders exposed in situ in a semi-industrial-scale digester. Long-term exposure was applied, for about two years, to low-carbon mortars and pastes based on slag cement, alkali-activated metakaolin, alkali-activated slag and supersulfated cements as well as mortars based on Portland and calcium aluminate cements in the liquid and the gas phases of the digester. The composition of the liquid and gas phase was monitored. After the exposure, the altered depths of the mortars were measured to establish a ranking of the performance of the different materials. The main degradation mechanisms of the various materials were also analysed by microscale analyses (scanning electron microscopy coupled to energy dispersive spectrometry, and X-ray diffraction).

# 1 Materials and methods

## 1.1 Binders

Cement pastes and mortars were manufactured from the following binders:

- an OPC CEM I 52,5 R Lafarge – Port la Nouvelle (CEM I), used as a reference binder;
- a slag cement, CEM III/B 42,5 N Lafarge – La Malle (CEM III) containing 71% of ground granulated blast furnace slag (GGBS);
- a calcium aluminate cement, Imerys Aluminates – Calcoat® RG (CAC);
- a metakaolin-based geopolymer (metakaolin from Argeco Développement; sodium silicate of modulus $SiO_2/Na_2O$ = 1.7, Betol 47T Na-Silicate from Wöllner; $SiO_2/Al_2O_3$ of the geopolymer = 3.6) (MKAA);
- an alkali-activated slag (AAS) from ECOCEM, the GGBS being activated by 10% of sodium silicate of modulus $SiO_2/Na_2O$ = 1.7, Betol 47T Na-Silicate from Wöllner;
- two supersulfated cements from ECOCEM (SSC2 and SSC3):
  - SSC2 contained >75% GGBS and 20% calcium sulfate;
  - SSC3 contained >75% GGBS, 20% calcium sulfate and an activator.

Chemical compositions of the binders are given in Table 1.

*Table 1. Oxide compositions of the binders in mass percentages and loss of ignition (l.o.i) (%) – ICP-OES analyses – n.d. = not detected*

| | $SiO_2$ | CaO | $Al_2O_3$ | $Fe_2O_3$ | $K_2O$ | $Na_2O$ | MgO | $TiO_2$ | $SO_3$ | $P_2O_5$ | l.o.i |
|---|---|---|---|---|---|---|---|---|---|---|---|

| | | | | | | | | | | | |
|---|---|---|---|---|---|---|---|---|---|---|---|
| **CEM I** | 20.00 | 66.20 | 4.85 | 2.64 | n.d. | 0.14 | 1.06 | 0.27 | 3.01 | 0.06 | 1.64 |
| **CEM III** | 30.00 | 48.80 | 9.48 | 2.78 | n.d. | 0.50 | 2.72 | 0.48 | 2.93 | 0.23 | 1.89 |
| **CAC** | 5.58 | 38.30 | 51.60 | 1.65 | 0.37 | 0.07 | 0.50 | 2.24 | 0.02 | 0.13 | 0.24 |
| **Metakaolin** | 68.10 | 1.38 | 25.60 | 3.58 | 0.32 | 0.03 | 0.22 | 1.22 | n.d. | 0.05 | 2.58 |
| **GGBS** | 33.19 | 41.75 | 11.16 | 0.58 | 0.55 | 0.31 | 7.38 | 0.77 | 0.06 | 0.03 | 0 |

The CEM I, CEM III, CAC, AAS and SSC pastes were poured with a water/binder ratio (W/B) of 0.30 and the associated mortars were poured with a W/B ratio of 0.40. The metakaolin-based alkali-activated pastes and mortars were manufactured according to Pouhet's procedure [21] by mixing metakaolin, liquid sodium silicate, water – and sand for the mortars. The precise designs of SSC are confidential. The pastes and mortars were mixed using an adaptation of the French standard NF EN 196-1 (using the water/binder ratios defined above but without sand for the pastes). Two types of moulds were used: cylindrical PVC moulds 75 mm high and 25 mm in diameter for CAC pastes only, and cylindrical PET plastic pillboxes 70 mm high and 35 mm in diameter for the other pastes and all the mortars. After casting, the PVC moulds were covered with plastic film and the pillboxes were closed with their lids. Immediately after pouring, a heat treatment was applied to the CAC specimens (pastes and mortars) in order to promote the conversion of the metastable hydrates $CAH_{10}$ and $CAH_8$ into stable hydrates $C_3AH_6$ [22]. For this purpose, the CAC specimens were placed in a climatic chamber at 35°C and 85% RH, and the temperature was gradually increased so as to reach 70°C after 3 hours. This temperature was maintained for a further 3 hours to allow the conversion. Finally, the specimens were placed in a storage chamber (20°C). The MKAA samples were removed from their moulds after 7 days of curing according to the recommendations of Pouhet [21]. Those based on CEM I and CAC underwent an endothermic cure of 28 days. Finally, the slag-based specimens, i.e. CEM III, AAS and SSC, had a longer 90-day endothermic cure in order to promote the formation of hydrates and therefore the reduction of porosity [23,24] as well as the development of their mechanical strength [25]. At the end of their curing period, all the samples were stored in closed plastic bags at 20°C. The mortars were sawn in half before exposure in order to double the number of samples.

## 1.2 Semi industrial scale digester

### 1.2.1 The SOLIDIA experimental platform

Samples were exposed to real anaerobic digestion conditions using the SOLIDIA platform at Bélesta-en-Lauragais (Haute-Garonne, France). This experimental platform was implemented by the CRITT GPTE[1] team of Toulouse Biotechnology Institute for research purposes. The experimental platform can be fed directly with biowaste or digestate from the CLER VERTS company, which specializes in the recovery of organic waste. Two tanks are dedicated to liquid anaerobic digestion on the SOLIDIA site. The digesters (2 m in diameter, about 3.5 m high, designed to contain 8 $m^3$) are made of polyethylene and insulated.

[1] CRITT GPTE: Centre Régional d'Innovation et de Transfert de Technologies, Génie des Procédés – Technologies Environnementales (Regional Centre for Innovation and Technology Transfer, Process Engineering – Environmental Technology)

### 1.2.2 Exposure conditions of the samples

- Distribution of the samples

The samples were exposed to both the liquid and the gas phases, in a single tank (Figure 1 (a)). To allow smooth circulation of the gas and liquid, the samples were placed in dishwasher cutlery baskets (Figure 1 (b)). The baskets were hung on two polypropylene structures set at different heights in the digester (Figure 1 (c)) (one structure for the gas phase and one for the liquid phase). The structures were then introduced into the digester through the manhole and fixed using chains (see Figure 1 (d)). The layout of the structures was designed considering the minimum and maximum filling levels and also the estimated height of the solid deposit fringe at the bottom of the tank, as shown in Figure 1 (d).

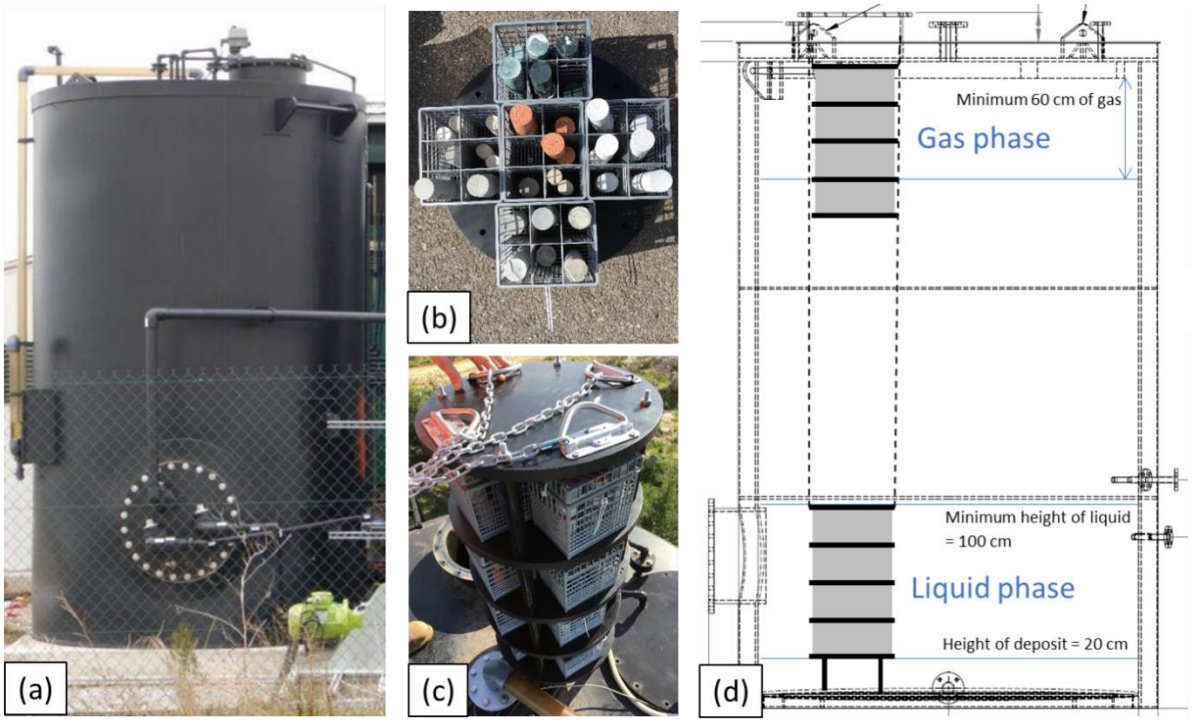


*Figure 1. (a) Semi industrial scale digester used for the in-situ exposure – SOLIDIA, Bélésta-en-Lauragais, (b) samples compartmented in dishwater baskets, (c) assembly of the baskets on a polypropylene structure, and (d) positioning of the basket structures in the digester*

The samples intended for the liquid phase were inserted in the digester on 18$^{th}$ March, 2019, whereas those for the gas phase were inserted on 6$^{th}$ June, 2019. The former were removed from the liquid phase on 24$^{th}$ June, 2021 whereas the latter were removed from the gas phase on 16$^{th}$ March, 2021. Thus the total exposure duration was approximately 2 years and 3 months in the liquid phase and 1 year and 10 months in the gas phase. The extracted samples were stored in closed plastic bags and kept in a storage chamber at 20°C until characterization.

- Digester feeding and composition of the liquid and gas phases

The CLER VERTS industrial digester is fed with biowaste from restaurants or unsold products from large and medium-sized retail outlets. It can treat vegetables, fruits, cereals, milk, meat, eggs, fish, and also agricultural waste such as manure and slurry [26]. The digestate produced is used to feed the SOLIDIA tanks. Usually, it is further degraded in a post-digester to produce

more methane (Figure 2). The use of a digestate as substrate leads to matter that is less biodegradable than biowaste, and thus to less aggressive conditions for the materials.

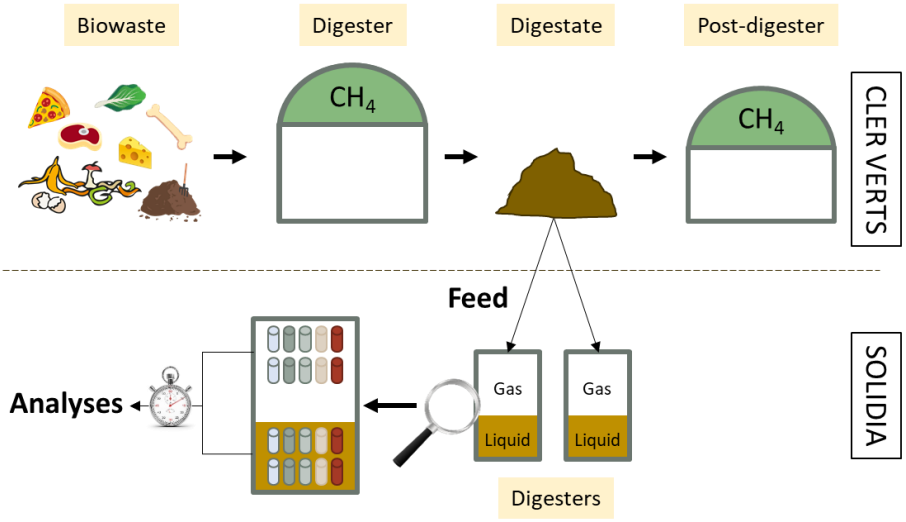


*Figure 2. Feeding of the SOLIDIA digesters*

The chemical compositions of the liquid phase were analysed on the following dates: 28/01/2020, 04/02/2020, 25/09/2020, 03/11/2020, 10/12/2020 and 21/06/2021. The results are shown in Table 2.

*Table 2. Composition of the liquid phase of the digester at six dates during the immersion (n.m. = not measured; n.d. = not detected < 1 mg/L)*

| Date | 28/01/2020 | 04/02/2020 | 25/09/2020 | 03/11/2020 | 10/12/2020 | 21/06/2021 |
|---|---|---|---|---|---|---|
| Duration of immersion | ≈ 10 months | ≈ 10.5 months | ≈ 18 months | ≈ 19.5 months | ≈ 20.5 months | ≈ 27 months |
| Inorganic carbon (gC/L) | n.m. | n.m. | 3.01 | 1.58 | n.m. | 3.69 |
| $[Cl^-]$ (mg/L) | 1165.3 | 1163.2 | 3267.0 | 1889.8 | 2417.8 | 3446.3 |
| $[NH_4^+]$ (mg/L) | 1487.4 | 1473.3 | 3589.4 | 3056.8 | 4001.9 | 3479.7 |
| $[Mg^{2+}]$ (mg/L) | 59.8 | 55.8 | 27.4 | 6.1 | 10.0 | 12.0 |
| $[K^+]$ (mg/L) | 1578.5 | 1528.3 | 1536.0 | 914.6 | 1264.9 | 1353.3 |
| $[Na^+]$ (mg/L) | 845.5 | 846.5 | 1113.0 | 840.4 | 880.2 | 1067.4 |
| $[Ca^{2+}]$ (mg/L) | 31.9 | 14.0 | 819.6 | 247.8 | 185.6 | 218.7 |
| pH | 7.75 | 8.04 | n.m. | n.m. | n.m. | n.m. |
| VFA tot (mg/L) | n.d. | n.d. | n.d. | n.d. | n.d. | n.d. |

The liquid phase of the digester was rich in $CO_2$ and contained high concentrations of $Cl^-$, $NH_4^+$ and $K^+$ (> 1 g/L), and $Na^+$ and $Ca^{2+}$ (several hundred mg/L). VFA concentrations were below the level of detection, which is consistent with the fact that VFA are continuously consumed in an efficient continuously fed digester. In previous laboratory experiments, lower ion concentrations were measured: $NH_4^+$ concentrations remained below 1 g/L, $Na^+$ concentrations were about 100 mg/L, and $K^+$ concentrations were several hundred mg/L [4,5,8,9]. $Mg^{2+}$ concentrations were similar both in situ and in laboratory experiments [4].

Carbon dioxide ($CO_2$) and methane ($CH_4$) contents were measured online during a previous campaign run in 2015 [27]. Variations in gas composition occurred in the tank, with $CO_2$ contents that varied from 25% to 60% and $CH_4$ contents that varied from 30% to 70% of the gas phase.

Moreover, the gas phase composition was analysed during the first year of exposition (March 2019 to March 2020). Figure 3 shows the $CH_4$ and $CO_2$ ratio (compared to the total amount of $CH_4$ and $CO_2$) in the gas phase of the digester during this period. No measurement of the $H_2S$ concentration was performed. In comparison with the previous measurements of 2015, low amount of $CO_2$ was observed in the tank. This could be explained by the presence of a large amount of cementitious pastes in the digester, which could have reacted with both the gaseous and dissolved $CO_2$.

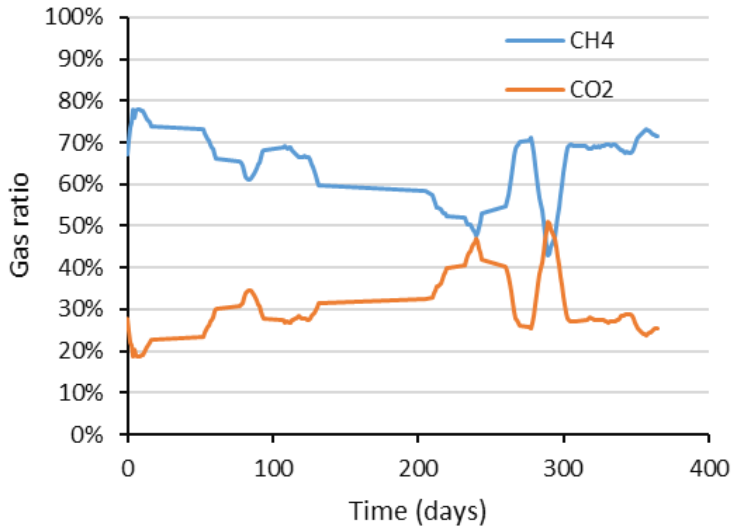


*Figure 3. $CH_4$ and $CO_2$ ratio (compared to the total amount of $CH_4$ and $CO_2$) in the gas phase of the digester between March 2019 and March 2020*

## 1.3 Analyses of the materials

The characterization of the deterioration of materials exposed to anaerobic digestion consisted of (i) the macroscopic analysis of the samples and (ii) the characterization of their microstructural, chemical and mineralogical alteration.

### 1.3.1 Macroscopic characterization: altered depths

The macroscopic analysis measured the altered depth (loss of alkalinity) by spraying phenolphthalein on two flat sawn sections of the sample. The colour change from violet (in the inner, alkaline zone of the sample) to transparent (in the outer layer in contact with the gas or liquid phase) indicated the altered depth. Two hours after the spraying, each side of a sample was scanned and the images were analysed using ImageJ software: the altered depths were measured at 32 points of measurement around the circumference. The average, 95% confidence intervals using Student's law, and minimum and maximum values of the 32 measurements are considered in the exploitation of the results.

### 1.3.2 Microscopic characterization

Thorough microscopic characterization was carried out in order to understand the various mechanisms of material deterioration. A diamond saw was used to collect circular slices from the samples for solid analyses. Quarter slices of mortars were prepared for Scanning Electron Microscopy (SEM) in backscattered electron mode (BSE) (JEOL JSM-LV, 15 kV) and Electron Probe Micro-Analysis (EPMA) (CamecaSXFive, 15 kV, 20 nA). The sections were embedded in an epoxy resin (Mecaprex Ma2+ from Presi), and dry polished using silicon carbide polishing disks (Presi; ESCIL, P800–22 µm, P1200–15 µm and P4000–5 µm). The flat, polished sections were then coated with carbon. The chemical composition changes were characterized using EPMA chemical profiles, from the surface to the core according to the distance to the surface. The analysis spots were chosen with particular care through point-by-point selection in order to analyse hydrated paste and not residual anhydrous grains. Trend curves, based on the analysis of three chemical composition profiles for each material, are used below to present the chemical modifications of the mortars (EPMA). The mineralogical alterations were assessed by qualitative X-Ray Diffraction analyses (XRD) (Bruker D8 Advance, Cu anti-cathode, 40 kV, 40 nA, 15 min, 2θ: 4 to 70°, 0.25 s per step in 0.02° increments) on the upper side of the paste samples. The plane side of the slices was first analysed, then the slice was successively abraded and analysed in order to characterize the mineralogical changes with depth, until sound paste was reached.

The degraded depths observed on the trend curves are not directly comparable with the phenolphthalein spray results since they rely on only a few chemical profiles that are not representative of the global composition of the material. This point is further addressed in the discussion.

# 2 Results

The materials were divided into three subclasses with regard to the nature of the binder: Portland cement-based materials (CEM I and CEM III), aluminium-rich materials (CAC and MKAA) and activated slag-based materials (AAS and SSC).

## 2.1 Deterioration of materials in the liquid phase

### 2.1.1 Altered depths of specimens

Figure 4 gives the altered depths of the different mortars exposed to the liquid phase of the digester for 2 years and 3 months. The average value of 32 measurements is provided for each mortar, together with the minimum and maximum values measured and the corresponding confidence intervals. The different material types are presented in increasing order of their degraded depth in order to establish their relative performance levels, with the CEM I-based mortar as the reference.

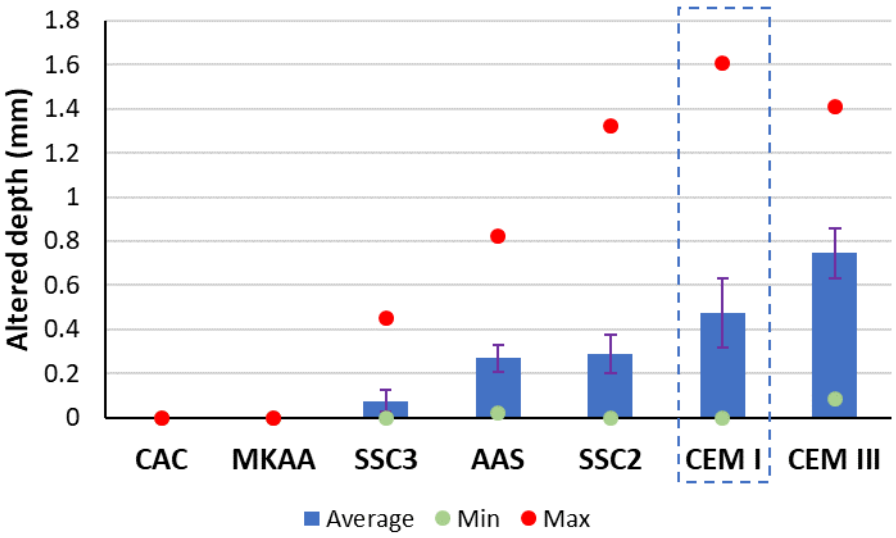


*Figure 4. Performance ranking of the mortars according to their altered depth after 2 years and 3 months of exposure to the liquid phase of the digester – blue dashed frame corresponds to the CEM I-based reference mortar*

Mortars made with CAC and MKAA did not show altered depths with this test (no colour change of the phenolphthalein on the whole cross section of the specimens). The SSC3, AAS and SSC2-based mortars had lower degraded depths than CEM I: respectively 0.075 ± 0.049 mm, 0.269 ± 0.063 mm, and 0.287 ± 0.088 mm versus 0.474 ± 0.156 mm. CEM III mortars presented the greatest degraded depths (0.745 ± 0.114 mm). The disparity between minimum and maximum values highlights a non-homogeneous alteration of the mortars on the circumference of the slices, probably linked with an uneven development of the biofilm on their surface [28].

### 2.1.2 Microstructural, chemical and mineralogical alteration of CEM I and CEM III mortars

Figure 5 summarizes the results of the SEM observations, the XRD analyses and the EPMA analyses.

The materials based on CEM I and CEM III mainly experienced dissolution and carbonation, calcite being the main crystallized mineralogical phase identified in the outer zone. The anhydrous phases were dissolved in the outer zone, where Ca leaching and a slight loss of density were observed in the SEM image. A sulfur enrichment occurred in the intermediate zone. Slight enrichments in $P_2O_5$ were observed close to the surface of the CEM I and CEM III mortars (up to 0.42% and 0.64% in mass, respectively). No major mineralogical change was observed deeper than 370 µm from the surface of the specimens. These mechanisms were similar to those previously observed in laboratory experiments [4,5].

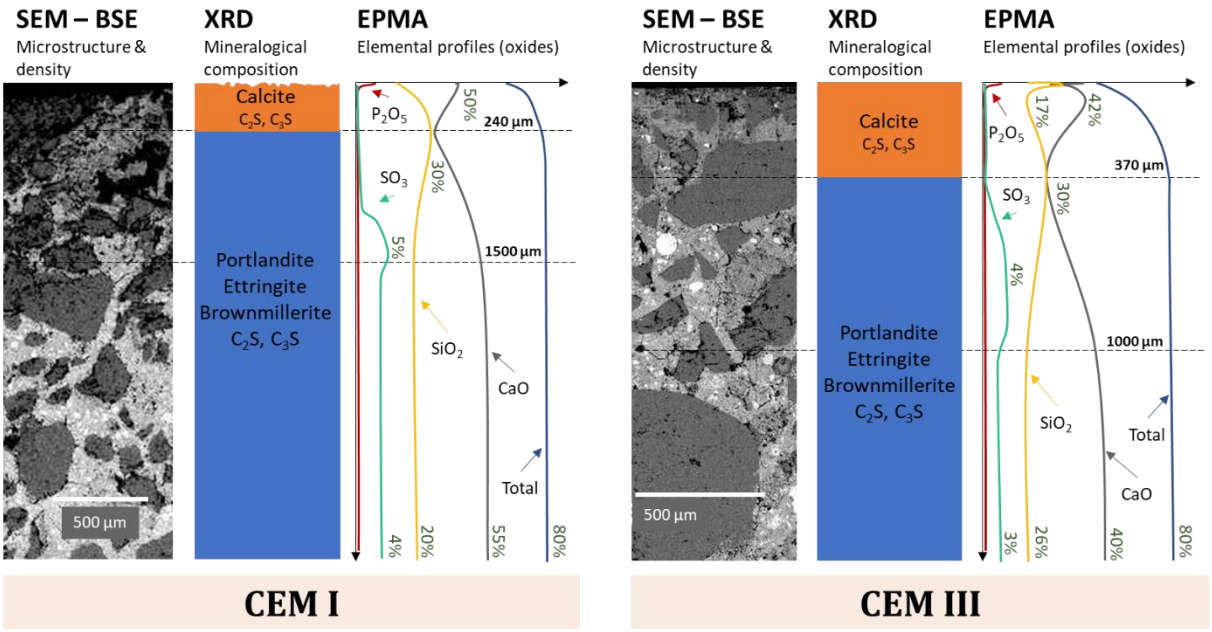


*Figure 5. BSE-SEM images and mineralogical and chemical compositions of the different zones of the CEM I and CEM III mortars after 2 years and 3 months of exposure in the liquid phase of a digester*

### 2.1.3 Microstructural, chemical, and mineralogical alteration of CAC and MKAA mortars

CAC mortar was slightly biodeteriorated but presented no major change in chemical and mineralogical compositions (Figure 6). A slight enrichment in $P_2O_5$ occurred near the surface (up to 0.28% in mass) and calcite precipitated.

A thin external carbonated layer was observed on the MKAA mortar (brighter layer in the SEM image) associated with the intensification of the calcite peaks in the XRD patterns and an enrichment in CaO coming from the liquid (since the geopolymer did not initially contain CaO) (EPMA). Under the carbonated layer, over 80 µm, the paste had a significantly lower density than the sound core. $K_2O$ (not shown) and $Na_2O$ were leached over 150 µm (from 3.4% to 1% and 0.7% to 0.3% respectively). The alteration of the material up to 350 µm deep resulted in the dissolution of the matrix, as in previous studies [4,5]. This deterioration was probably due to the acidic component of the liquid medium since similar dissolution has already been observed during acid attacks in other studies [29–31].

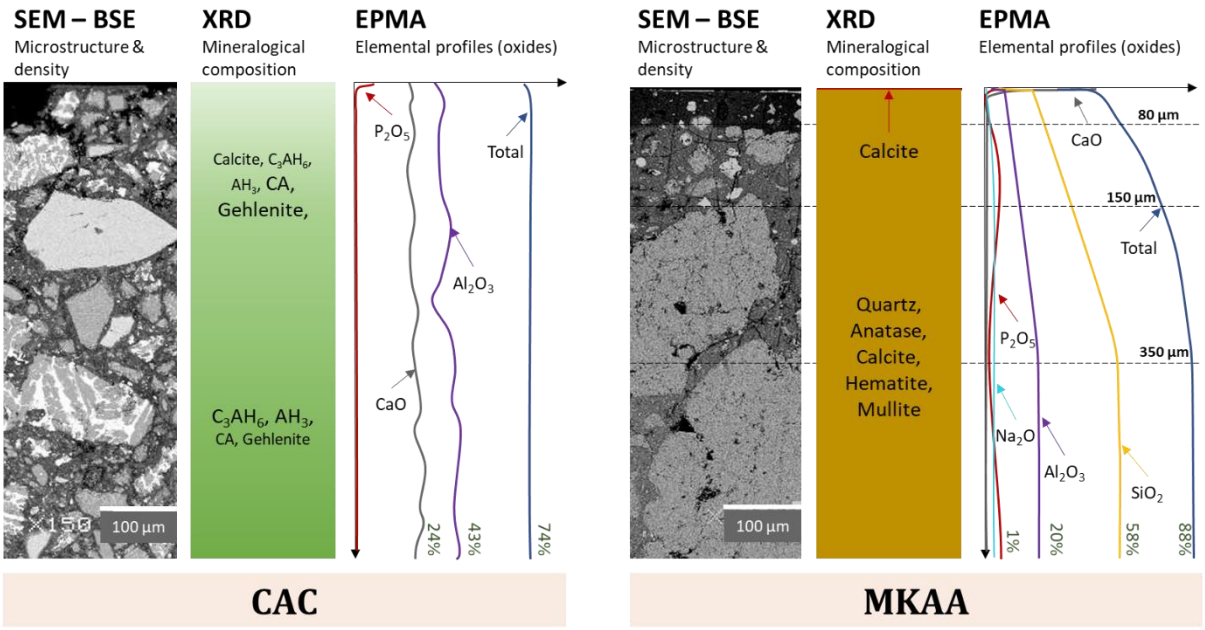


*Figure 6. BSE-SEM images and mineralogical and chemical compositions of the different zones of the CAC and MKAA mortars after 2 years and 3 months of exposure in the liquid phase of a digester*

### 2.1.4 Microstructural, chemical and mineralogical alteration of AAS, SSC2 and SSC3 mortars

Figure 7 shows the mineralogical and chemical alterations (analysed by XRD and EPMA respectively) and SEM images of the AAS, SSC2 and SSC3 samples.

According to the mineralogical and chemical analyses, the alteration mechanism of the AAS material was mainly surface carbonation, expressed by the intensification of the calcite signal (XRD) in the outer layer and the precipitation of calcite and vaterite. However, no major change in the mortar chemical composition was spotted. A slight enrichment in $P_2O_5$ (up to 0.8% at 18 µm deep) was observed in the outer layer.

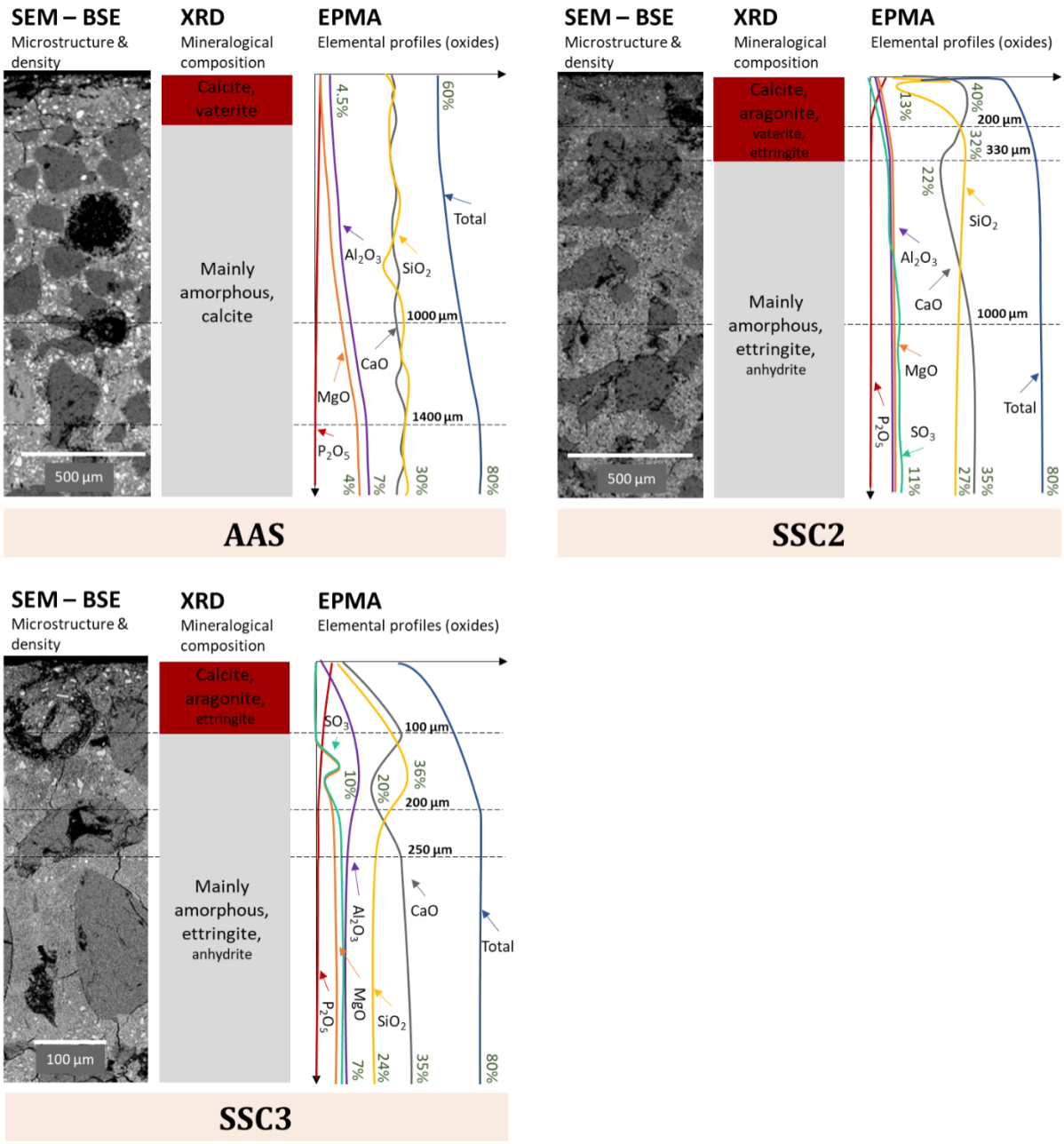


*Figure 7. BSE-SEM images and mineralogical and chemical compositions of the different zones of the AAS, SSC2 and SSC3 mortars after 2 years and 3 months of exposure in the liquid phase of a digester*

XRD analyses showed the precipitation of the crystallized calcium carbonate phases in the outer layer of the SSC2 and SSC3 mortars. Calcite and aragonite precipitated in both mortars whereas vaterite was identified only in SSC3. This is consistent with the chemical composition profiles, which showed a slight decalcification in depth, and then an increase in the calcium oxide content associated with the decrease in the contents of other oxides up to the surface of the mortars, corresponding to carbonation and leaching. The density of the mortars decreased close to the surface (darker zones in the SEM image). An enrichment in phosphorus was observed in the outer layer (up to 0.5% at 38 µm deep for SSC2 and up to 0.6% at 20 µm deep for SSC3).

Thus, the degradation phenomena observed on the three slag-based materials (AAS, SSC2 and SSC3) were mainly surface carbonation and leaching, with a slight enrichment in phosphorus in the outermost few tens of microns. However, according to the chemical composition profiles, the sensitivities of the slag-based materials to the attack were significantly different: SSC3 had a degraded depth of 250 µm, SSC2 of 1000 µm and AAS of 1400 µm.

## 2.2 Deterioration of materials in the gas phase

### 2.2.1 Altered depth of specimens

Figure 8 shows the altered depths of the different mortars that were exposed to the gas phase of the digester (average values of the 32 lengths measured for each), together with the minimum value and the maximum value measured, and the corresponding confidence intervals. The results are presented in increasing order of degraded depth so as to establish the relative performances of the samples, the CEM I-based mortar being used as a reference. Unfortunately, the liquid level rose during the in situ exposure and the CAC-based mortars were submerged, so could not be studied and compared with the other samples. As the SSC3 mortar was the most efficient slag-based material in the liquid phase, it was chosen to be studied in the gas phase.

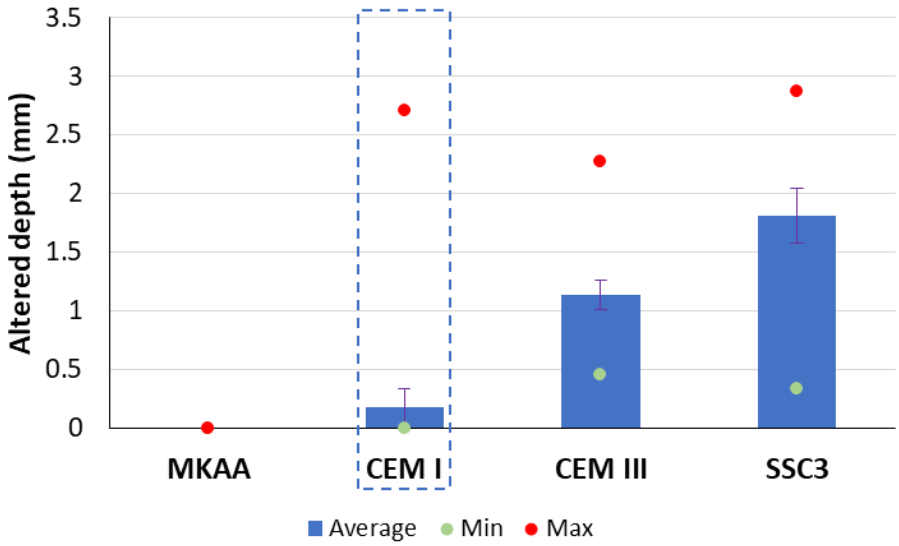


*Figure 8. Performance ranking of the mortars according to their altered depth after 1 year and 10 months of exposure to the gas phase of the digester – blue dashed frame corresponds to the CEM I-based reference mortar*

As for the specimens immersed in the liquid phase, this test highlighted no altered depth on the MKAA-based mortar, and the CEM III-based mortar showed deeper altered depth (1.135 ± 0.122 mm) than the CEM I-based mortar (0.183 ± 0.158 mm). However, in the gas phase, the SSC3 mortar showed lower performance than the CEM I-based mortar, with significantly higher altered depth (1.813 ± 0.231 mm). A great disparity in the distribution of the alteration depth was noted.

### 2.2.2 Microstructural, chemical and mineralogical alteration of CEM I and CEM III mortars

The structural, chemical and mineralogical analyses of the CEM I-based mortar (Figure 9) highlighted carbonation in the surface layer, with the precipitation of calcite and aragonite, needle-shaped aragonite crystals [32] being observed on the SEM images inside the porosity.

Few anhydrous grains remained in this external zone, which was less dense than the core. From 850 µm to 1500 µm deep, an enrichment in sulphur was observed in the chemical composition profile, associated with a denser paste and microcracks in the SEM image. This could correspond to a local precipitation of secondary ettringite. No phosphorous enrichment was spotted. The mortar was sound from 1500 µm deep.

The alteration of CEM III-based mortar was very similar to that of the CEM I-based mortar. A whitish deposit was visible (to the naked-eye) on the surface of the sample, which corresponded to a thin layer of calcium carbonate unevenly covering its surface (SEM image). Moreover, large, needle-shaped precipitates were observed in places. XRD analyses showed the presence of calcite and aragonite. The external 2000 µm thick zone was less dense than the core of the specimen with few remaining anhydrous grains. From 2000 µm to 2500 µm deep, the matrix showed higher density, microcracking, and an enrichment in sulfur, up to 15% at some places, which could be the sign of ettringite precipitation in this area. The mortar was sound from 2500 µm deep. Note that, for this sample, the degradation was not homogeneous and probably depended on the uneven covering of the surface by calcium carbonate crystals, which may have prevented the penetration of aggressive agents by clogging the porosity.

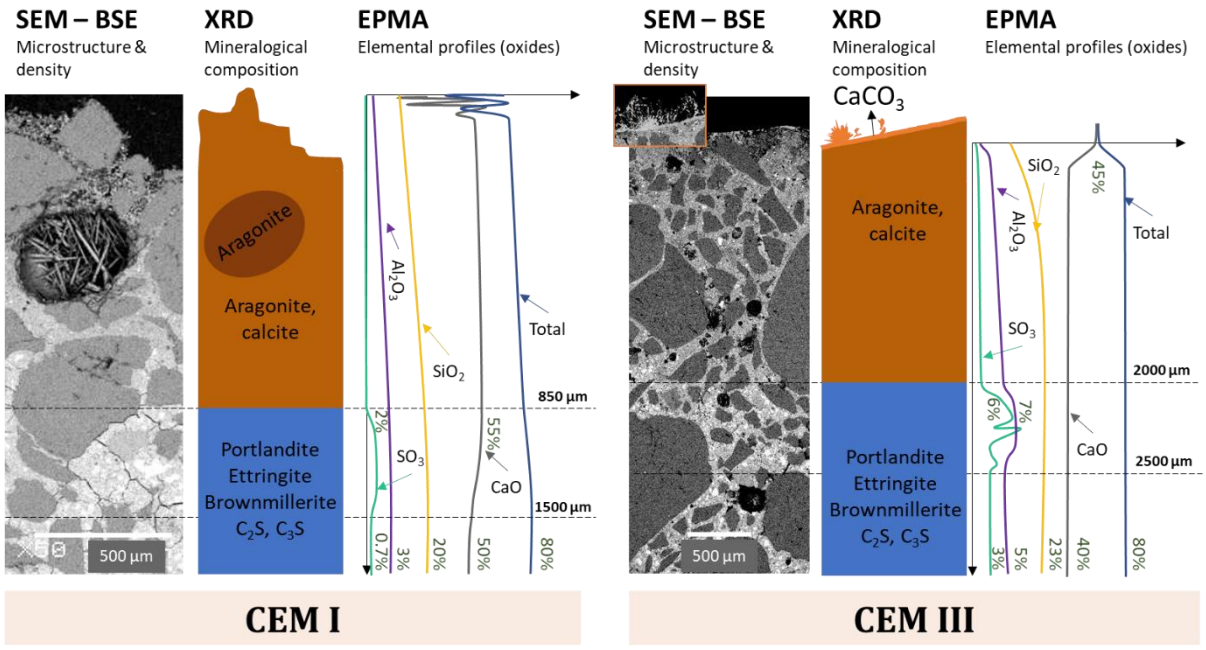


*Figure 9. BSE-SEM images and mineralogical and chemical compositions of the different zones of the CEM I and CEM III mortars after 1 year and 10 months in the gas phase of a digester*

### 2.2.3 Microstructural, chemical and mineralogical alteration of MKAA mortar

Figure 10 shows the structural, mineralogical and chemical composition of the MKAA mortar after its exposure to the gas phase of the digester. Only slight leaching was observed from the chemical composition profile, illustrated by a less dense matrix (SEM image). $Na_2O$ was slightly leached (from 1.5% to 1%) on the outer 140 µm (not shown for easier reading of the graph). No mineralogical change was observed by XRD analyses. The material was sound from 300 µm deep.

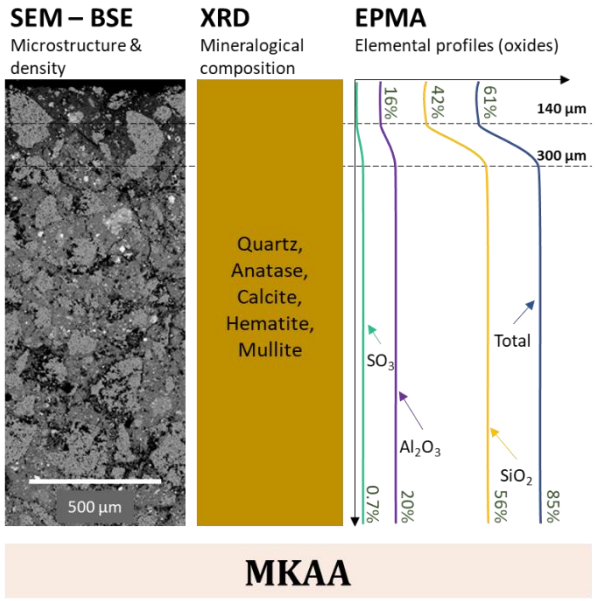


*Figure 10. BSE-SEM images and mineralogical and chemical compositions of the different zones of the MKAA mortar after 1 year and 10 months in the gas phase of a digester*

### 2.2.4 Microstructural, chemical and mineralogical alteration of SSC3

Several zones could be observed in the SSC3-based mortar exposed to the gas phase (Figure 11). Beyond 2400 µm, the specimen was unaltered, with the chemical composition corresponding to a sound SSC paste. Microcracks were present but were probably due to the high ettringite content of the sound hydrated binder. From 2400 µm to 1000 µm deep, the EPMA chemical analyses showed a slow decrease of the total oxides content, a slow decalcification associated with a sulfur enrichment and an increase of the relative $SiO_2$ content. In the SEM image, this zone showed a lower density than the sound core, and microcracks. The external zone (up to 1000 µm) showed a poorly dense matrix, where calcite and aragonite were the only crystallized phases detected. Sulfate and magnesium were completely leached, while the calcium content was high (about 35%) and the total oxide content was stable, due to carbonation.

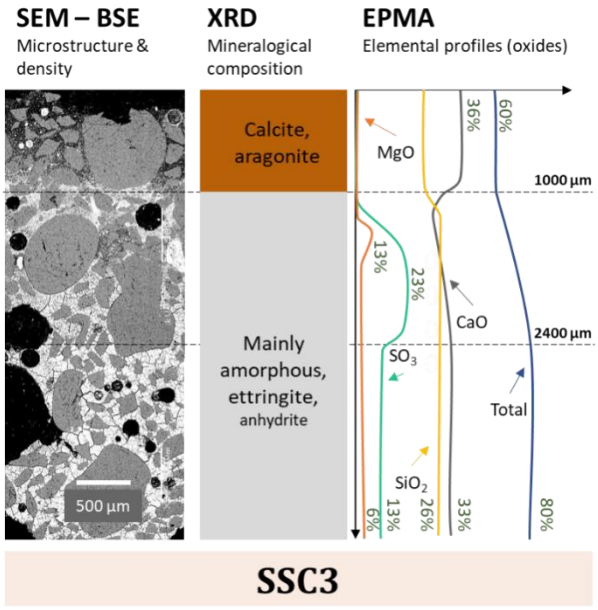


*Figure 11. BSE-SEM images and mineralogical and chemical compositions of the different zones of the SSC3 mortar after 1 year and 10 months in the gas phase of a digester*

# 3 Discussion

## 3.1 Deterioration mechanisms

### 3.1.1 Liquid phase

In the liquid phase, the main degradation phenomena were leaching and carbonation, as calcium carbonates, mainly calcite but also aragonite and vaterite, precipitated in the outer layers of all the mortar. The joint presence of the three crystallized polymorphs of calcium carbonates could be due to the high RH and temperature in the environments considered, but also to the carbonation of C-S-H and ettringite [33–38]. This carbonation was linked to the high concentration of dissolved $CO_2$ in the liquid phase due to the microbial production of $CO_2$ in the liquid, and in the biofilm, in direct contact with the materials. Moreover, the sulfur enrichment observed for CEM I, CEM III and SSC3 mortars was probably due to the precipitation of non-expansive secondary ettringite. This phenomenon is classically observed in materials exposed to leaching because of the diffusion of sulfates from the altered zone inwards [4,39,40].

An enrichment in phosphorus was systematically observed on the surface of the mortars but no phosphorus-rich crystallized phases were identified by XRD. Moreover, the depth of phosphorus penetration was not the same for all the materials. Since this phosphorus enrichment was probably due to the penetration of exogenous phosphorus from the fermenting biowaste [41], the depth of penetration may have been related to the diffusion properties of the cementitious matrix.

Despite an intense carbonation and the associated dissolution of the initial Ca-bearing phases and precipitation of calcium carbonates, there was no significant variation in the calcium content inside the materials. This may have been due to the high calcium content of the

surrounding liquid medium (several hundred mg/L, Table 2) which did not favour the leaching of calcium from the matrix to the external medium.

The degradations observed under anaerobic digestion conditions in situ were similar to those observed in laboratory studies [4,5,8,9,42], where the authors showed a combination of leaching and carbonation, with surface phosphorus enrichment for CEM I and CEM III pastes. In the laboratory and in situ, the CAC and MKAA specimens were the best preserved under these aggressive conditions. In the present study, the AAS and SSC materials also underwent a combination of carbonation and leaching, and were better preserved than the Portland-based materials CEM I and CEM III. As the composition of the liquid was not the same as in the laboratory experiments (the substrate nature and the frequency of substrate supply were different), this could have resulted in different biofilm coverage (density, variety and number of microorganisms), different amounts of metabolites in contact with the materials and different deterioration patterns. The composition of the biofilm and its thickness were not studied in the different configurations, which makes it impossible to establish possible correlations.

### 3.1.2 Gas phase

The main degradation phenomenon in the gas phase was carbonation. However, the carbonation was more intense than in the liquid phase since greater carbonated depths and well-crystallized aragonite and calcite were observed in the SEM images, in the pores and on the surface of the materials. This carbonation was linked to a medium not saturated with water, but with high RH, and to the high proportion of $CO_2$ in the gas phase (up to 60%).

In contrast with the observations of Koenig and Dehn [6], no precipitate of elementary or amorphous sulfur was identified on the surface of the materials, nor was any secondary precipitation of gypsum observed at depth. As the digester was fed with digestate, it is likely that the sulfur had already been converted into $H_2S$ in the previous industrial digester, which could explain the absence of $H_2S$ in the semi-industrial scale one. Moreover, unlike in Koenig and Dehn's study, there was no treatment of $H_2S$ by microaeration here and therefore no possibility of oxidizing the potential residual $H_2S$ into sulfuric acid. This low-$H_2S$ environment is similar to what can be encountered in industrial digesters degrading biowaste containing little sulfur or in post-digesters.

## 3.2 Relative performances of cementitious binders

The altered depths observed on the chemical composition profiles contradict the classification obtained by phenolphthalein spraying. This could be explained by the very great heterogeneity of the degradations along the surface of the material, highlighted by the disparity of the measured altered depths. Thus, a reliable performance ranking cannot be made on the basis of localized chemical composition profiles. For this reason, only the altered depths obtained by phenolphthalein spraying were used for the performance ranking, although this indicator is not particularly suitable for alkali-activated materials [43].

In the liquid medium, where carbonation and leaching were predominant, the materials were ranked in increasing order of performance as follows: CEM III < CEM I < SSC2 < AAS < SSC3 < CAC & MKAA. In the gas phase of anaerobic digestion, where conditions were favourable for

intense carbonation, the materials studied were classified in increasing order of performance: SSC3 < CEM III < CEM I < MKAA.

The difference in the composition of the media led to a different ranking according to the type of environment, in particular for AAS- and SSC-based materials, which were less degraded than Portland cements in the liquid phase, but not in the gas phase.

The use of slag is known to increase the chemical resistance of materials to leaching and acid attack by reducing the calcium and portlandite contents of the binder in favour of C-(A-)S-H [44,45]. High acid resistance is also reported for alkali-activated slag-based materials and is also due to their specific C-(N-)A-S-H (or C-(K-)A-S-H) phase assemblage [29,46–50]. However, the properties specific to the use of slag (reduced or no portlandite content, higher proportion of C-(A-)S-H of lower Ca/Si ratio) are not beneficial to the resistance to carbonation. Under carbonation, the C-(A-)S-H are decalcified by decreasing the Ca/Si ratio and that can lead to a silicate polymerization and to the formation of an amorphous silica gel, together with precipitation of calcium carbonates. For extensive carbonation, this can result in significant shrinkage, loss of cohesion, increased porosity, cracking and a decrease of the micro-mechanical properties, with increased diffusion coefficients [51–58]. Moreover, the density of ettringite-based materials (SSC) tends to decrease as a result of carbonation since a large amount of bound water is released during carbonation reactions [59,60]. On the contrary, the carbonation of CEM I paste does not seem to have had a negative effect on the durability of the material. In the presence of portlandite, the precipitation of calcium carbonates clogs the porosity, which leads to a decrease in pore volume and pore connection of the paste [53,61]. These phenomena explain both the good behaviour of AAS- and SSC-based materials in the liquid phase and their less good behaviour in the $CO_2$-rich gas phase [62–64]. Besides, the better performance of SSC3 compared to SSC2 showed that an improved design (addition of an activator) can significantly improve the performance of the material. Finally, the poorer performance of CEM III in the liquid phase was probably due to the combined sensitivity of slag cement to carbonation, and a relatively low leaching resistance (compared to AAS- and SSC-based materials). On the one hand, the presence of portlandite in the CEM III paste, a phase sensitive to leaching (compared to C-A-S-H), was not beneficial for the material. On the other hand, portlandite could have acted as a sacrificial phase during the carbonation reaction but it may have been dissolved by leaching before its combination with carbonates forming clogging calcium carbonates.

In contrast, the CAC and MKAA materials had the lowest degradation after exposure, whether in a carbonating and leaching environment (CAC & MKAA) or in an intense carbonation environment (MKAA only). This is in accordance with previous studies showing that CAC-based and MKAA materials performed best in anaerobic digestion conditions [4,5,8,20]. The good performance of CAC-based samples could be due to the lower colonization of the material by microorganisms (compared with OPC-based materials) [8,65–68] and/or to the beneficial formation of an aluminium gel ($AH_3$) on the surface, which is known to be stable at moderately acidic pH, i.e. up to pH 4 [15,69]. The degradation of the MKAA materials in the liquid phase was mainly expressed by the dissolution of the matrix, as classically encountered during acid attacks [29–31,50]. The sodium content of the matrix was lower in the liquid phase than in the

gas phase, indicating that alkalis leaching was probably higher in the liquid medium. However, no silica gel acting as a barrier layer was identified in the present study. This was probably due to the neutral pH of the liquid medium, since silica gel precipitates at low pH in short-term exposure [50,70], but also to the presence of calcium in solution, leading to the precipitation of calcium carbonates. In the gas phase, the carbonation only marginally affected the MKAA mortars. The overall good performance of MKAA materials was probably due to its chemical and mineralogical composition and also to the stability of its geopolymer framework due to its high $SiO_2/Al_2O_3$ ratio [66]. However, a reservation can be made regarding the characterization of the MKAA geopolymer, since alkalis from the pore solution were not analysed and sodium carbonates were not measured. Actually, the alkalis in these matrices are mainly in the pore solution and are rapidly carbonated due to the high connected porosity of the material [71]. The carbonation products are very soluble and therefore offer very little protection. In order to enable full understanding of the alteration of the materials, an additional study of their transfer properties would be necessary, in particular for MKAA, which is known to have high, interconnected porosity [72].

### 3.3 Normative context

The non-harmonized European standard EN 206+A2/CN [73] and the French information document FD P 18-011 [74] classify chemically aggressive environments in three classes of increasing aggressiveness, XA1 to XA3, especially for waters and for gases in wet conditions. The aggressiveness of water depends on its concentration of aggressive agents – aggressive $CO_2$, $SO_4^{2-}$, $Mg^{2+}$, $NH_4^+$, and low total alkali strength (TAC) – and its pH, whereas the aggressiveness of gases in wet environments depends on their $SO_2$ and $H_2S$ concentrations.

The liquid medium of neutral pH was $CO_2$-rich (1 – 3 gC/L) and contained high ammonium concentrations (1000 – 4000 mg/L), low magnesium concentrations (6 – 60 mg/L), and no sulfate. The attack by this medium resulted in the leaching and carbonation of the materials. The attack by the gas medium, mainly composed of $CO_2$ (25% to 60%) and $CH_4$ (30% to 70%) led to carbonation of the matrices. While the main alterations observed in this study resulted from carbonation of the binders, $CO_2$ is not considered aggressive to the cementitious matrix according to the standards. Moreover, in these two $CO_2$-rich environments, CEM III mortars were more deteriorated than CEM I mortars, while French standards and guidelines recommend the use of blast furnace cement in environments that are chemically very aggressive (XA3) [73–75], such as agricultural structures. Thus, it might be relevant to consider the additional effect of $CO_2$ on the recommended cements, for liquid or gaseous aggressive environments.

## Conclusion and perspectives

This study assessed the performance of different low carbon mortars, together with a reference Portland cement-based mortar, toward anaerobic digestion media. Although the liquid and gaseous media were very different, it appears that the major mechanism in both environments and for all materials was carbonation on the surface. In view of these results, it is very likely that (i) the liquid phase contained few VFA and that (ii) the gas phase contained little or no $H_2S$ during the exposure of the materials.

In addition, the phenolphthalein tests allowed the materials' performance to be ranked and, in the current conditions of exposure:

- CAC and MKAA materials showed the best behaviour, whether in the liquid or the gas phase of the digester;
- Because of their good behaviour in an acid environment but their sensitivity to carbonation, the activated slag-based materials (AAS and SSC) behaved better than Portland-based materials (CEM I and CEM III) in the liquid phase but not in the gas phase;
- Due to the sensitivity of slag-Portland cements to carbonation, in the gas phase and in the liquid phase, slag cement (CEM III) was more degraded than Portland cement (CEM I).

Thus, future work could focus on the great variability of the compositions of the liquid and gaseous phases over time, according to the inputs and depending on the installations. In addition, and considering the high cost of using CAC or MKAA concrete, it would be interesting to (i) study the use of cementitious coatings by assessing their transfer properties and (ii) focus on improving the design of the least expensive low-carbon materials, such as AAS and SSC, so that they can be used industrially and resist both the gas and the liquid phases. Finally, consideration should be given to reviewing the standards and recommendations concerning the various binders to be used in these media, in particular by considering the great variability of the media compositions.

## Acknowledgements

The authors thank the CLER VERTS company and Evrard Mengelle for his help.

## Credit author statement

Marie Giroudon: Conceptualization, methodology, investigation, supervision, writing – original draft, visualization.

Cédric Patapy: Conceptualization, methodology, validation, writing: review & editing, supervision.

Matthieu Peyre Lavigne: Conceptualization, methodology, validation, resources, writing: review & editing, supervision

Mialitiana Andriamiandroso: Investigation

Robin Cartier: Investigation

Céline Bacquié: Investigation

Ludovic André: Conceptualization, resources

Simon Dubos: Investigation, resources

Sébastien Pommier: Investigation, resources, writing: review & editing

Xavier Lefevbre: Resources, project administration, writing: review & editing

Martin Cyr: Resources, writing: review & editing

Alexandra Bertron: Conceptualization, methodology, validation, writing: review & editing, supervision, project administration, funding acquisition.

## Compliance with Ethical Standards

Funding: This study was funded by the French National Research Agency (ANR) (project BIBENdOM – ANR – 16 – CE22 – 001 DS0602).

Conflict of Interest: The authors declare that they have no conflict of interest.

## References

[1] ADEME, Fiche technique : Méthanisation, (2015). https://www.ademe.fr/methanisation-fiche-technique.

[2] E.S.A. Nathalie Bachmann, 8 - Design and engineering of biogas plants, in: A. Wellinger, J. Murphy, D. Baxter (Eds.), Biogas Handb., Woodhead Publishing, 2013: pp. 191–211. https://doi.org/10.1533/9780857097415.2.191.

[3] J.N. Meegoda, B. Li, K. Patel, L.B. Wang, A Review of the Processes, Parameters, and Optimization of Anaerobic Digestion, Int. J. Environ. Res. Public. Health. 15 (2018) 2224. https://doi.org/10.3390/ijerph15102224.

[4] M. Giroudon, M. Peyre Lavigne, C. Patapy, A. Bertron, Blast-furnace slag cement and metakaolin based geopolymer as construction materials for liquid anaerobic digestion structures: Interactions and biodeterioration mechanisms, Sci. Total Environ. 750 (2021) 141518. https://doi.org/10.1016/j.scitotenv.2020.141518.

[5] M. Giroudon, C. Perez, M. Peyre Lavigne, B. Erable, C. Lors, C. Patapy, A. Bertron, Insights into the local interaction mechanisms between fermenting broken maize and various binder materials for anaerobic digester structures, J. Environ. Manage. 300 (2021) 113735. https://doi.org/10.1016/j.jenvman.2021.113735.

[6] A. Koenig, F. Dehn, Biogenic acid attack on concretes in biogas plants, Biosyst. Eng. 147 (2016) 226–237. https://doi.org/10.1016/j.biosystemseng.2016.03.007.

[7] C. Perez, C. Lors, P. Floquet, B. Erable, Biodeterioration kinetics and microbial community organization on surface of cementitious materials exposed to anaerobic digestion conditions, J. Environ. Chem. Eng. 9 (2021) 105334. https://doi.org/10.1016/j.jece.2021.105334.

[8] C. Voegel, M. Giroudon, A. Bertron, C. Patapy, M. Peyre Lavigne, T. Verdier, B. Erable, Cementitious materials in biogas systems: Biodeterioration mechanisms and kinetics in CEM I and CAC based materials, Cem. Concr. Res. 124 (2019) 105815. https://doi.org/10.1016/j.cemconres.2019.105815.

[9] C. Voegel, A. Bertron, B. Erable, Mechanisms of cementitious material deterioration in biogas digester, Sci. Total Environ. 571 (2016) 892–901. https://doi.org/10.1016/j.scitotenv.2016.07.072.

[10] C. Voegel, N. Durban, A. Bertron, Y. Landon, B. Erable, Evaluation of microbial proliferation on cementitious materials exposed to biogas systems, Environ. Technol. (2019) 1–11. https://doi.org/10.1080/09593330.2019.1567610.

[11] C. Magniont, M. Coutand, A. Bertron, X. Cameleyre, C. Lafforgue, S. Beaufort, G. Escadeillas, A new test method to assess the bacterial deterioration of cementitious

materials, Cem. Concr. Res. 41 (2011) 429–438. https://doi.org/10.1016/j.cemconres.2011.01.014.
[12] K. Obileke, S. Mamphweli, E.L. Meyer, G. Makaka, N. Nwokolo, Development of a Mathematical Model and Validation for Methane Production Using Cow Dung as Substrate in the Underground Biogas Digester, Processes. 9 (2021) 643. https://doi.org/10.3390/pr9040643.
[13] M. Vénuat, Relations entre la carbonatation du béton et les phénomènes de la corrosion des armatures du béton, Ann. L'ITBTP. (1978) 42–47.
[14] A. Aboulela, M.P. Lavigne, A. Buvignier, M. Fourré, M. Schiettekatte, T. Pons, C. Patapy, O. Robin, M. Bounouba, E. Paul, A. Bertron, Laboratory Test to Evaluate the Resistance of Cementitious Materials to Biodeterioration in Sewer Network Conditions, Materials. 14 (2021) 686. https://doi.org/10.3390/ma14030686.
[15] A. Buvignier, C. Patapy, M. Peyre Lavigne, E. Paul, A. Bertron, Resistance to biodeterioration of aluminium-rich binders in sewer network environment: Study of the possible bacteriostatic effect and role of phase reactivity, Cem. Concr. Res. 123 (2019) 105785. https://doi.org/10.1016/j.cemconres.2019.105785.
[16] J. Herisson, E.D. van Hullebusch, M. Moletta-Denat, P. Taquet, T. Chaussadent, Toward an accelerated biodeterioration test to understand the behavior of Portland and calcium aluminate cementitious materials in sewer networks, Int. Biodeterior. Biodegrad. 84 (2013) 236–243. https://doi.org/10.1016/j.ibiod.2012.03.007.
[17] Islander Robert L., Devinny Joseph S., Mansfeld Florian, Postyn Adam, Shih Hong, Microbial Ecology of Crown Corrosion in Sewers, J. Environ. Eng. 117 (1991) 751–770. https://doi.org/10.1061/(ASCE)0733-9372(1991)117:6(751).
[18] C.D. Parker, Mechanics of Corrosion of Concrete Sewers by Hydrogen Sulfide, Sew. Ind. Wastes. 23 (1951) 1477–1485.
[19] C.D. Parker, The corrosion of concrete. 2. The function of Thiobacillus concretivorus (nov. spec.) in the corrosion of concrete exposed to atmospheres containing hydrogen sulphide, Aust. J. Exp. Biol. Med. Sci. 23 (1945) 91–98.
[20] M. Giroudon, M. Peyre Lavigne, C. Patapy, A. Bertron, Biodeterioration mechanisms and kinetics of SCM and aluminate based cements and AAM in the liquid phase of anaerobic digestion, MATEC Web Conf. 199 (2018) 02003. https://doi.org/10.1051/matecconf/201819902003.
[21] R. Pouhet, Formulation and durability of metakaolin-based geopolymers, PhD Thesis, Université de Toulouse, Université Toulouse III - Paul Sabatier, 2015. http://thesesups.ups-tlse.fr/2802/ (accessed December 18, 2017).
[22] K. Scrivener, J.-L. Cabiron, R. Letourneux, High-performance concretes from calcium aluminate cements, Cem. Concr. Res. 29 (1999) 1215–1223. https://doi.org/10.1016/S0008-8846(99)00103-9.
[23] A. Attari, C. McNally, M.G. Richardson, A combined SEM–Calorimetric approach for assessing hydration and porosity development in GGBS concrete, Cem. Concr. Compos. 68 (2016) 46–56. https://doi.org/10.1016/j.cemconcomp.2016.02.001.
[24] C. Perlot, J. Verdier, M. Carcassès, Influence of cement type on transport properties and chemical degradation: application to nuclear waste storage, Mater. Struct. 39 (2006) 511–523.
[25] A. Bougara, C. Lynsdale, N.B. Milestone, The influence of slag properties, mix parameters and curing temperature on hydration and strength development of slag/cement blends,

643 Constr. Build. Mater. 187 (2018) 339–347.
644 https://doi.org/10.1016/j.conbuildmat.2018.07.166.
645 [26] CLER VERTS, CLER VERTS. (n.d.). https://www.cler-verts.fr/ (accessed October 9, 2022).
646 [27] C. Voegel, Impact biochimique des effluents agricoles et agroindustriels sur les
647 structures/ouvrages en béton dans la filière de valorisation par méthanisation (ou
648 digestion anaérobie), PhD Thesis, Institut National Polytechnique de Toulouse (INP
649 Toulouse), 2017. http://www.theses.fr/2017INPT0044.
650 [28] C. Voegel, A. Bertron, B. Erable, Biodeterioration of cementitious materials in biogas
651 digester, Matér. Tech. 103 (2015) 202. https://doi.org/10.1051/mattech/2015023.
652 [29] T. Bakharev, Resistance of geopolymer materials to acid attack, Cem. Concr. Res. 35
653 (2005) 658–670. https://doi.org/10.1016/j.cemconres.2004.06.005.
654 [30] O. Burciaga-Díaz, J.I. Escalante-García, Strength and Durability in Acid Media of Alkali
655 Silicate-Activated Metakaolin Geopolymers, J. Am. Ceram. Soc. 95 (2012) 2307–2313.
656 https://doi.org/10.1111/j.1551-2916.2012.05249.x.
657 [31] N. Ukrainczyk, O. Vogt, Geopolymer leaching in water and acetic acid, RILEM Tech. Lett.
658 5 (2020) 163–173. https://doi.org/10.21809/rilemtechlett.2020.124.
659 [32] D. Chakrabarty, S. Mahapatra, Aragonite crystals with unconventional morphologies, J.
660 Mater. Chem. 9 (1999) 2953–2957. https://doi.org/10.1039/a905407c.
661 [33] P. López-Arce, L.S. Gómez-Villalba, S. Martínez-Ramírez, M. Álvarez de Buergo, R. Fort,
662 Influence of relative humidity on the carbonation of calcium hydroxide nanoparticles and
663 the formation of calcium carbonate polymorphs, Powder Technol. 205 (2011) 263–269.
664 https://doi.org/10.1016/j.powtec.2010.09.026.
665 [34] K. Ndiaye, M. Cyr, S. Ginestet, Durability and stability of an ettringite-based material for
666 thermal energy storage at low temperature, Cem. Concr. Res. 99 (2017) 106–115.
667 https://doi.org/10.1016/j.cemconres.2017.05.001.
668 [35] B. Chen, M. Horgnies, B. Huet, V. Morin, K. Johannes, F. Kuznik, Comparative kinetics
669 study on carbonation of ettringite and meta-ettringite based materials, Cem. Concr. Res.
670 137 (2020) 106209. https://doi.org/10.1016/j.cemconres.2020.106209.
671 [36] E. Drouet, S. Poyet, P. Le Bescop, J.-M. Torrenti, X. Bourbon, Carbonation of hardened
672 cement pastes: Influence of temperature, Cem. Concr. Res. 115 (2019) 445–459.
673 https://doi.org/10.1016/j.cemconres.2018.09.019.
674 [37] E.T. Stepkowska, J.L. Pérez-Rodríguez, M.J. Sayagués, J.M. Martínez-Blanes, Calcite,
675 vaterite and aragonite forming on cement hydration from liquid and gaseous phase, J.
676 Therm. Anal. Calorim. 73 (2003) 247–269. https://doi.org/10.1023/A:1025158213560.
677 [38] R. Ševčík, M. Pérez-Estébanez, A. Viani, P. Šašek, P. Mácová, Characterization of vaterite
678 synthesized at various temperatures and stirring velocities without use of additives,
679 Powder Technol. 284 (2015) 265–271. https://doi.org/10.1016/j.powtec.2015.06.064.
680 [39] A. Bertron, J. Duchesne, G. Escadeillas, Attack of cement pastes exposed to organic acids
681 in manure, Cem. Concr. Compos. 27 (2005) 898–909.
682 https://doi.org/10.1016/j.cemconcomp.2005.06.003.
683 [40] P. Faucon, F. Adenot, J.F. Jacquinot, J.C. Petit, R. Cabrillac, M. Jorda, Long-term behaviour
684 of cement pastes used for nuclear waste disposal: review of physico-chemical
685 mechanisms of water degradation, Cem. Concr. Res. 28 (1998) 847–857.
686 https://doi.org/10.1016/S0008-8846(98)00053-2.
687 [41] H. Xu, S. Yun, C. Wang, Z. Wang, F. Han, B. Jia, J. Chen, B. Li, Improving performance and
688 phosphorus content of anaerobic co-digestion of dairy manure with aloe peel waste

using vermiculite, Bioresour. Technol. 301 (2020) 122753. https://doi.org/10.1016/j.biortech.2020.122753.
[42] A. Bertron, M. Peyre Lavigne, C. Patapy, B. Erable, Biodeterioration of concrete in agricultural, agro-food and biogas plants: state of the art and challenges, RILEM Tech. Lett. 2 (2017) 83–89. https://doi.org/10.21809/rilemtechlett.2017.42.
[43] O. Ojedokun, P. Mangat, Suitability of phenolphthalein indicator method for alkali activated concrete, in: V. Caprai, H.J.H. Brouwers (Eds.), Eindhoven University of Technology, Eindhoven, The Netherlands, 2019: pp. 363–372. https://research.tue.nl/en/publications/proceedings-icsbm-2019-2nd-international-conference-of-sustainabl.
[44] Y. Elakneswaran, E. Owaki, S. Miyahara, M. Ogino, T. Maruya, T. Nawa, Hydration study of slag-blended cement based on thermodynamic considerations, Constr. Build. Mater. 124 (2016) 615–625. https://doi.org/10.1016/j.conbuildmat.2016.07.138.
[45] B. Lothenbach, K. Scrivener, R.D. Hooton, Supplementary cementitious materials, Cem. Concr. Res. 41 (2011) 1244–1256. https://doi.org/10.1016/j.cemconres.2010.12.001.
[46] C. Shi, J.A. Stegemann, Acid corrosion resistance of different cementing materials, Cem. Concr. Res. 30 (2000) 803–808. https://doi.org/10.1016/S0008-8846(00)00234-9.
[47] J. Blaakmeer, Diabind: An alkali-activated slag fly ash binder for acid-resistant concrete, Fuel Energy Abstr. 5 (1995) 336.
[48] S.A. Bernal, R. Mejía de Gutiérrez, J.L. Provis, Engineering and durability properties of concretes based on alkali-activated granulated blast furnace slag/metakaolin blends, Constr. Build. Mater. 33 (2012) 99–108. https://doi.org/10.1016/j.conbuildmat.2012.01.017.
[49] A. Koenig, A. Herrmann, S. Overmann, F. Dehn, Resistance of alkali-activated binders to organic acid attack: Assessment of evaluation criteria and damage mechanisms, Constr. Build. Mater. 151 (2017) 405–413. https://doi.org/10.1016/j.conbuildmat.2017.06.117.
[50] G. Gluth, C. Grengg, N. Ukrainczyk, F. Mittermayr, M. Dietzel, Acid resistance of alkali-activated materials: recent advances and research needs, RILEM Tech. Lett. 7 (2022) 58–67. https://doi.org/10.21809/rilemtechlett.2022.157.
[51] N. Li, N. Farzadnia, C. Shi, Microstructural changes in alkali-activated slag mortars induced by accelerated carbonation, Cem. Concr. Res. 100 (2017) 214–226. https://doi.org/10.1016/j.cemconres.2017.07.008.
[52] M.Á. Sanjuán, E. Estévez, C. Argiz, D. del Barrio, Effect of curing time on granulated blast-furnace slag cement mortars carbonation, Cem. Concr. Compos. 90 (2018) 257–265. https://doi.org/10.1016/j.cemconcomp.2018.04.006.
[53] B. Šavija, M. Luković, Carbonation of cement paste: Understanding, challenges, and opportunities, Constr. Build. Mater. 117 (2016) 285–301. https://doi.org/10.1016/j.conbuildmat.2016.04.138.
[54] S. Steiner, B. Lothenbach, T. Proske, A. Borgschulte, F. Winnefeld, Effect of relative humidity on the carbonation rate of portlandite, calcium silicate hydrates and ettringite, Cem. Concr. Res. 135 (2020) 106116. https://doi.org/10.1016/j.cemconres.2020.106116.
[55] M. Nedeljković, B. Šavija, Y. Zuo, M. Luković, G. Ye, Effect of natural carbonation on the pore structure and elastic modulus of the alkali-activated fly ash and slag pastes, Constr. Build. Mater. 161 (2018) 687–704. https://doi.org/10.1016/j.conbuildmat.2017.12.005.
[56] F. Puertas, M. Palacios, T. Vázquez, Carbonation process of alkali-activated slag mortars, J. Mater. Sci. 41 (2006) 3071–3082. https://doi.org/10.1007/s10853-005-1821-2.

[57] P.H.R. Borges, J.O. Costa, N.B. Milestone, C.J. Lynsdale, R.E. Streatfield, Carbonation of CH and C–S–H in composite cement pastes containing high amounts of BFS, Cem. Concr. Res. 40 (2010) 284–292. https://doi.org/10.1016/j.cemconres.2009.10.020.
[58] V.T. Ngala, C.L. Page, Effects of carbonation on pore structure and diffusional properties of hydrated cement pastes, Cem. Concr. Res. 27 (1997) 995–1007. https://doi.org/10.1016/S0008-8846(97)00102-6.
[59] C. Xiantuo, Z. Ruizhen, C. Xiaorong, Kinetic study of ettringite carbonation reaction, Cem. Concr. Res. 24 (1994) 1383–1389. https://doi.org/10.1016/0008-8846(94)90123-6.
[60] Q. Zhou, F.P. Glasser, Kinetics and mechanism of the carbonation of ettringite, Adv. Cem. Res. 12 (2000) 131–136. https://doi.org/10.1680/adcr.2000.12.3.131.
[61] J. Han, Y. Liang, W. Sun, W. Liu, S. Wang, Microstructure Modification of Carbonated Cement Paste with Six Kinds of Modern Microscopic Instruments, J. Mater. Civ. Eng. 27 (2015) 04014262. https://doi.org/10.1061/(ASCE)MT.1943-5533.0001210.
[62] S.A. Bernal, J.L. Provis, B. Walkley, R. San Nicolas, J.D. Gehman, D.G. Brice, A.R. Kilcullen, P. Duxson, J.S.J. van Deventer, Gel nanostructure in alkali-activated binders based on slag and fly ash, and effects of accelerated carbonation, Cem. Concr. Res. 53 (2013) 127–144. https://doi.org/10.1016/j.cemconres.2013.06.007.
[63] S.A. Bernal, J.L. Provis, D.G. Brice, A. Kilcullen, P. Duxson, J.S.J. van Deventer, Accelerated carbonation testing of alkali-activated binders significantly underestimates service life: The role of pore solution chemistry, Cem. Concr. Res. 42 (2012) 1317–1326. https://doi.org/10.1016/j.cemconres.2012.07.002.
[64] Y. Xie, T. Sun, Z. Shui, C. Ding, W. Li, The impact of carbonation at different CO2 concentrations on the microstructure of phosphogypsum-based supersulfated cement paste, Constr. Build. Mater. 340 (2022) 127823. https://doi.org/10.1016/j.conbuildmat.2022.127823.
[65] C. Lors, J. Aube, R. Guyoneaud, F. Vandenbulcke, D. Damidot, Biodeterioration of mortars exposed to sewers in relation to microbial diversity of biofilms formed on the mortars surface, Int. Biodeterior. Biodegrad. 130 (2018) 23–31. https://doi.org/10.1016/j.ibiod.2018.03.012.
[66] C. Grengg, N. Ukrainczyk, G. Koraimann, B. Mueller, M. Dietzel, F. Mittermayr, Long-term in situ performance of geopolymer, calcium aluminate and Portland cement-based materials exposed to microbially induced acid corrosion, Cem. Concr. Res. 131 (2020) 106034. https://doi.org/10.1016/j.cemconres.2020.106034.
[67] M. Peyre Lavigne, A. Bertron, L. Auer, G. Hernandez-Raquet, J.-N. Foussard, G. Escadeillas, A. Cockx, E. Paul, An innovative approach to reproduce the biodeterioration of industrial cementitious products in a sewer environment. Part I: Test design, Cem. Concr. Res. 73 (2015) 246–256. https://doi.org/10.1016/j.cemconres.2014.10.025.
[68] E. Dalod, A. Govin, R. Guyonnet, P. Grosseau, C. Lors, D. Damidot, Influence of the chemical composition of mortars on algal biofouling, in: K.L. Fentiman C.H.;. Mangabhai, R.J.;. Scrivener (Ed.), Int. Conf. Calcium Aluminates, IHS BRE Press, Palais des Papes, Avignon, France, 2014: pp. 523–534.
[69] H. Fryda, F. Saucier, S. Lamberet, K. Scrivener, D. Guinot, La durabilité des bétons d'aluminates de calcium, in: Durabilité Bétons, Presse de l'ENCP, 2008: pp. 767–823.
[70] M. Mainguy, C. Tognazzi, J.-M. Torrenti, F. Adenot, Modelling of leaching in pure cement paste and mortar, Cem. Concr. Res. 30 (2000) 83–90. https://doi.org/10.1016/S0008-8846(99)00208-2.

[71] R. Pouhet, M. Cyr, Carbonation in the pore solution of metakaolin-based geopolymer, Cem. Concr. Res. 88 (2016) 227–235. https://doi.org/10.1016/j.cemconres.2016.05.008.
[72] R. Pouhet, M. Cyr, R. Bucher, Influence of the initial water content in flash calcined metakaolin-based geopolymer, Constr. Build. Mater. 201 (2019) 421–429. https://doi.org/10.1016/j.conbuildmat.2018.12.201.
[73] AFNOR, NF EN 206+A2/CN. Concrete - Specification, performance, production and conformity - National addition to the standard NF EN 206+A2, Paris, France, 2022.
[74] AFNOR, FD P18-011. Concrete - Definition and classification of chemically aggressive environments - Recommendations for concrete mix design, Paris, France, 2022.
[75] CIMbéton, Guide de prescription des ciments pour des constructions durables. Cas des bétons coulés en place, 2009. https://www.infociments.fr/ciments/t47-guide-de-prescription-des-ciments-pour-des-constructions-durables (accessed March 1, 2018).